A review in titanium-zirconium binary alloy for use in dental implants: Is there an ideal Ti-Zr composing ratio?☆

Qian Zhao, Takeshi Ueno *, Noriyuki Wakabayashi

Advanced Prosthodontics, Department of Masticatory Function Rehabilitation, Graduate School of Medical and Dental Sciences, Tokyo Medical and Dental University, Tokyo, Japan

ARTICLE INFO

ABSTRACT

Binary titanium-zirconium alloys have been studied as promising alternatives for Ti implants. The commercial Ti-15Zr alloy (Roxolid, Straumann) has been the major subject of numerous binary Ti-Zr alloys-related studies and has gained wide recognition in laboratory studies and clinical practices. However, binary Ti-Zr alloys of other composition ratios are still being investigated by researchers. This review aims to provide information on the potential of binary Ti-Zr alloys other than Ti-15Zr as implant materials in terms of mechanical strengths, chemical or electrochemical corrosion resistance capabilities, and biological performances. In addition, in this review, the Ti-15Zr alloy is discussed only when compared with other binary Ti-Zr alloys. From the included 26 studies, it is confirmed that the mechanical, chemical, electrochemical, and biological properties of Ti-Zr alloys are related to the Ti and Zr composition ratio in the alloy, phase, manufacturing process, and surface treatment. Among the studied alloys, α-or α′ phase-Ti-5 wt, 45 wt/30at, and 50 wt. %Zr exhibited relatively more promising results for further investigation. More research is necessary to evaluate the potential for future use of these materials for implants.

Contents

1. Introduction

Titanium is the most widely used biomaterial for dental implants. Titanium has admittedly excellent osteointegration ability, but its mechanical strength or corrosion resistance is insufficient in some cases, where reduced-dimension implants are required or the

---

corrosive environment is severe, like those containing chlorides or fluorides. To improve the properties of titanium implants, the binary titanium-zirconium alloy has emerged as a good candidate for implant use, particularly in these demanding conditions [1]. The development and successful commercial use of Ti-15 % or 13–17 %Zr alloy (Roxolid, Institute Straumann, Basel, Switzerland) have made binary Ti-Zr alloys very appealing to researchers, resulting in many studies. In the process of retrieving papers using our search strategy, 113 studies of Ti-15 % or 13–17 %Zr alloy (Roxolid) were obtained. Fig. 1 shows how these studies are distributed across different categories. A small part of these Roxolid studies are briefly stated here: The tensile strength and fatigue endurance limit of Ti-15 %Zr alloy were found to be higher than those of grade 4 titanium, without reducing the tensile elongation or the fracture toughness [2]. On both Ti SLA and Ti-13–17 %Zr SLA surfaces, the osteoblastic differentiation and maturation markers of human MSCs and osteoblasts were enhanced to a comparable extent [3]. The SLActive Ti and Ti-13–17 %Zr surfaces exhibited increased cell attachment, proliferation, and osteoblastic differentiation compared to the SLA surfaces [4]. The long-term vertical osteoconductivity of SLActive Ti-Zr dental implants is comparable to those of Ti implants in rabbits [5]. It was found that the removal torque values for the Ti-Zr group were statistically higher than those of the Ti group in both the sham-aged and the ovariectomized rabbits, reflecting an increased bone quality around the Ti-Zr implants [6]. Clinically, it was reported that Ti-Zr narrow-diameter implants in the anterior or premolar regions with single-implant crown restoration did not differ from the Ti regular-diameter implants over a 3-year period in the change of marginal bone loss and mucosa levels and the occurrence of complications [7].

Despite the pioneering success of the Ti-15Zr alloy, investigation of the ideal composition ratio of Ti and Zr has never ceased. Moreover, several review papers [8,9] summarize the state of the research on binary Ti-Zr alloys for dental implants, most of which undoubtedly cite the Roxolid Ti-15Zr alloy. However, there are still no reviews that intentionally exclude the Roxolid Ti-15Zr alloy to focus on the state of the research on binary Ti-Zr alloys with other compositions. Therefore, this study aims to (1) summarize the state of research on other binary Ti-Zr alloys and (2) screen out the binary Ti-Zr alloys (if there are any) that possess superior mechanical, chemical, electrochemical, or biological properties than commercially pure titanium or Ti-15Zr alloy.

2. Materials and methods

The literature survey was conducted by searching PubMed and Web of Science databases by title, abstract, and topic for publications published before October 11, 2022, with search strategies: (1) 'Ti-Zr' OR 'Ti-Zr alloy' OR 'TiZr' OR 'TiZr alloy' OR 'titanium-zirconium' OR 'titanium-zirconium alloy' OR 'titanium zirconium' OR 'titanium zirconium alloy' AND 'dental implant.' The publication language was limited to English. The exclusion criteria were as follows: (1) studies examining Ti-Zr alloys that also contain other elements; (2) studies examining Ti-Zr alloys for non-endosseous dental screws such as abutments and crowns; (3) studies on ceramic zirconia; (4) studies examining Zr element coating on Ti or additional coatings on Ti-Zr substrates; (5) imaging artefact studies; (6) studies where the unit (wt. % or at. %) of composition ratio is not described; (7) studies on finite element analysis; (8) studies with unclear Ti and Zr composition ratio; (9) studies that specialize in Roxolid implants; (10) studies in which a comparison of a binary Ti-Zr alloy with Ti or other binary Ti-Zr alloys is not provided; and (11) review articles or (12) articles that could not be accessed in their entirety. The inclusion criteria were studies examining the surface, mechanical, chemical, and electrochemical characteristics or biological performances. A first screening by reading abstracts and a second screening by reading full texts were performed to remove any articles that met the exclusion criteria. A citation search was performed to make the study's inclusion more complete. A flow diagram of the literature survey process is shown in Fig. 2.

3. Results

Following the initial search strategies, 581 articles from PubMed and 519 articles from Web of Science were retrieved, and duplicates were removed by using Mendeley and manual check, leaving 932 articles processed for the first screening by reading the titles and abstracts. For the second screening, 56 articles were selected. After
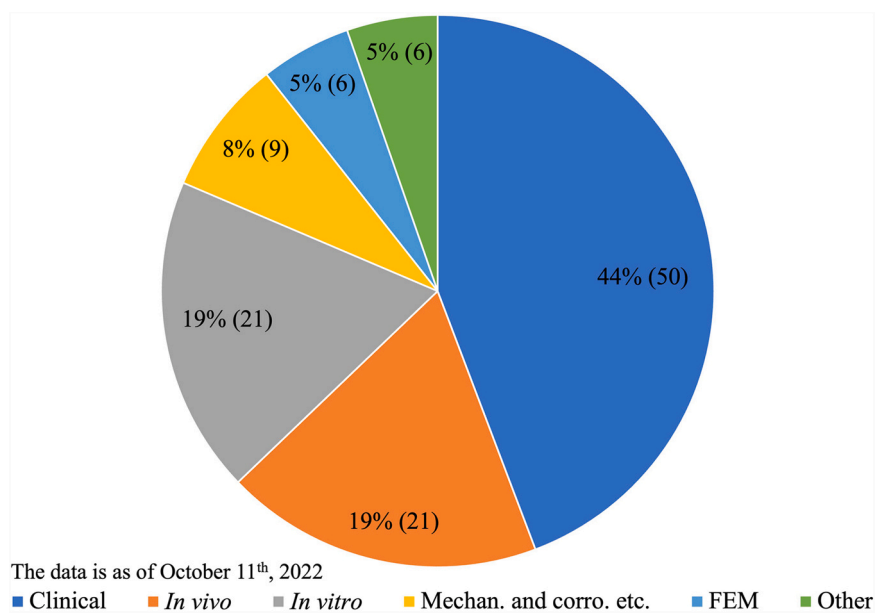

Fig. 1. Distribution chart of studies related to commercial Roxolid implants. Microstructure, mechanical, physical, or chemical/electrochemical corrosion resistance studies: 9; *in vitro* cellular studies: 21; *in vivo* animal studies: 21; clinical studies: 50; finite element analysis studies: 6; others like magnetic resonance imaging: 6.
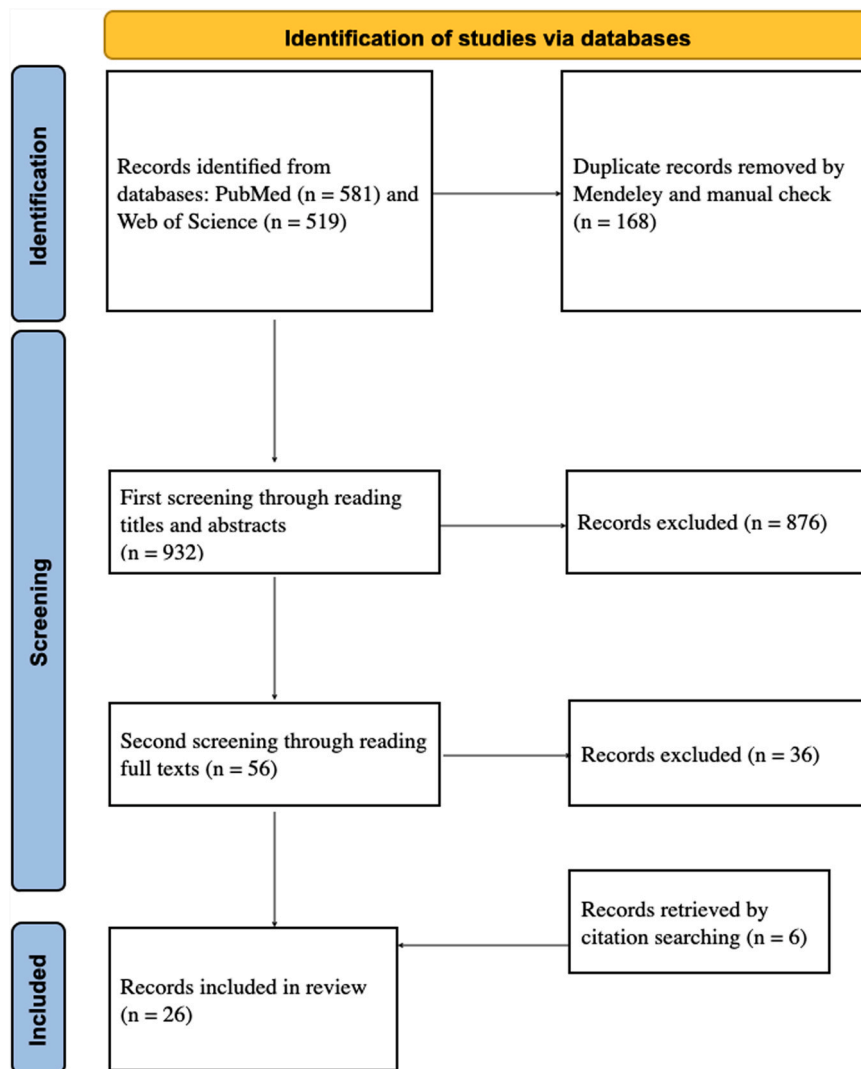
Identification of studies via databases

Identification

| Records identified from databases: PubMed (n = 581) and Web of Science (n = 519) | → | Duplicate records removed by Mendeley and manual check (n = 168) |

Screening

| First screening through reading titles and abstracts (n = 932) | → | Records excluded (n = 876) |

| Second screening through reading full texts (n = 56) | → | Records excluded (n = 36) |

| | | Records retrieved by citation searching (n = 6) |

Included

| Records included in review (n = 26) |

Fig. 2. Literature inclusion process (adapted from PRISMA 2020 flow diagram).

reading the full texts, 20 studies were included. Additional 6 studies were identified by citation searching. Finally, 26 articles were included in this review.

Of the 26 studies, 20 examined the microstructure (n = 14), mechanical (n = 14), and chemical or electrochemical (n = 13) properties; 11 analyzed *in vitro* outcomes, and 2 studies are about *in vivo* experiments. The results are summarized in Table 1. The same or similar composition ratios are listed in adjacent rows and the studies by the same or related researchers are placed in the same-colour cells. In summary, the studied composition ratios of binary Ti-Zr alloys cover almost the entire range: Ti-5–95 wt. %Zr and Ti-10–90at. %Zr. Two methods of pre-material production were used: ingot metallurgy and powder metallurgy. The subsequent processing steps included swaging, forging, rolling, heat treatment, and casting. The cooling conditions included furnace, air, and water cooling. The produced alloys presented different phase compositions: α, α', $\alpha + \beta$, and β, which had their respective microscopic characteristic microstructures. Regardless of the various phase compositions and microstructures of these alloys, among these composition ratios, α or α' phase-Ti-5 wt, 45 wt/30at, and 50 wt. %Zr were the most well-supported ones after being evaluated by different research teams. The optimal composition ratio could not be further derived because these alloys were not examined in the same study.

4. Discussion

4.1. Phase compositions/microstructures, zirconium contents, and manufacturing procedures

Titanium has two crystallographic forms: α and β phases. At room temperature, commercially pure titanium exhibits a hexagonal close-packed (hcp)-structured α phase. At 883 °C, Ti transforms from an hcp α phase to a body-centered cubic (bcc)-structured β phase [10]. Alloying with additional elements and thermomechanical processing can affect the transformation of both crystallographic variations. According to their effect on the stability of the α and β phases, alloying elements can be categorized as α-stabilizers (Al, O, N, and Ga), which increase the transformation temperature, and β-stabilizers (Mo, V, W, and Ta), which decrease the transformation temperature [10]. Zirconium is considered a neutral element that also displays a transition in the solid-state from the low-temperature hcp α phase to the high-temperature bcc β phase. Titanium and zirconium are completely miscible in all phases. Alloying Zr with Ti forms substitutional solid solutions. Although the α/β transformation in pure Zr occurs at 862 °C [11], which is very close to that of Ti, the onset temperature of the α/β transformation varies with the composition in Ti-Zr alloys. The effect of Zr concentration on the Ms temperature ($\beta \rightarrow \alpha$ on cooling) is shown in Fig. 3 (phase diagram of

Table 1
The included literature.

Author (year)	Alloys	Manufacturing process	Phase composition	Surface treatment	Mechanical strengths	Anti-corrosion capabilities	Biological properties
Correa et al. (2013) [26]	Ti-5Zr, 10Zr, 15Zr (wt%)	Melting → hot swaging	α'	—	Elastic modulus: Ti-15Zr > Ti, Ti-10Zr > Ti-5Zr	—	Cytotoxicity: Ti-Zr alloys were slightly higher than Ti
Cordeiro et al. (2017) [23]	Ti-5Zr, 10Zr (wt%)	Melting → hot swaging → heat treatment → air-cooling	α	—	Microhardness: Ti-5Zr > -10Zr > Ti-6Al-4V; Elastic modulus: Ti-10Zr > -5Zr > Ti	Corrosion resistance: Ti-5, -10Zr > Ti	Ti-Zr alloys had comparable albumin adsorption with Ti
Cordeiro et al. (2018) [24]	Ti-5Zr, 10Zr, 15Zr (wt%)	Melting → hot swaging → heat treatment → air-cooling	α	Double acid etching	Machined surfaces: Hardness: Ti-5Zr>10, 15Zr>Ti-6Al-4V; Elastic modulus: Ti-10Zr>Ti-15Zr>Ti-5Zr>Ti; Stiffness: Ti-10Zr>Ti, Ti-5, 15Zr. Double etched surface hardness: Ti-15Zr > -5Zr > -10Zr > Ti	Highest corrosion resistance: Ti-15Zr	Double acid etching was beneficial for cell adhesion and proliferation on Ti-Zr alloys
Barão et al. (2021) [25]	Ti-5Zr, 10Zr, 15Zr (wt%)	Melting → hot swaging → heat treatment → air-cooling	α*	—	Microhardness: Ti-5, 10, 15Zr > Ti; Elastic modulus: Ti-10Zr > -15Zr > -5Zr > Ti; Stiffness: Ti-10Zr > Ti, Ti-5, 15Zr	Corrosion resistance: Ti-5Zr, -15Zr > -10Zr	—
Han et al. (2014) [27]	Ti-5Zr, 10Zr, 15Zr, 20Zr (wt%)	Melting → heat treatment → furnace-cooling → air-cooling	α	—	Microhardness: Ti-15 > -10 > -5, 20Zr > Ti	Highest corrosion resistance: Ti-15Zr	—
Moreno et al. (2013) [20]	Ti-20wt%Zr	Vacuum semi-levitation melting and casting	α + β	—	UTS, 0.2% YS, and EL: Ti-20Zr > Ti; Young's modulus: Ti-20Zr < Ti	Corrosion resistance: Ti-20Zr > Ti	—
Kim et al. (2009) [18]	Ti-10, 20, 30, 40Zr (wt%)	Melting → heat treatment	α + β	Anodization	—	Highest corrosion resistance: Ti-40Zr	—
Ho et al. (2008) [21]	Ti-10, 20, 30, 40Zr (wt%)	Melting → casting	α	—	Ti-40Zr showed the highest hardness, bending strength, and elastic recovery angle	—	—
Hsu et al. (2009) [19]	Ti-60, 70, 80, 90Zr (wt%)	Melting → casting	Ti-90Zr: α'; Ti-70, -80Zr: α' + β; Ti-60Zr: β	—	Ti-90Zr showed the greatest elastic recovery capability	—	—
Cui et al. (2015) [1]	Ti-60, 80Zr (wt%)	Melting → hot forging → heat treatment → water-cooling	—	Thermal oxidization	Hardness: oxidized Ti-Zr alloys > unoxidized Ti-Zr alloys; Wear resistance: oxidized Ti-60Zr > oxidized Ti-80Zr > Ti-60, 80Zr	Corrosion resistance: oxidized Ti-60Zr > oxidized Ti-80Zr > Ti-60Zr > Ti-80Zr	—
Cui et al. (2019) [29]	Ti-50Zr, commercial Ti-16Zr (wt%)	Melting → hot forging → Ti-16Zr: rotary forging (room temperature); Ti-50Zr: hot rolling and air-cooling	Ti-50Zr: α'; commercial Ti-16Zr: α	SLA: sandblasting and dual acid etching	Yield strength, ultimate tensile strength, and fatigue limit: Ti-50Zr > Ti-16Zr; fatigue limit: SLA Ti-50Zr > Ti-16Zr > SLA Ti-16Zr > Ti	—	—
Kobayashi et al. (1995) [17]	Ti-20, 25, 30, 35, 40, 45, 50, 55, 60, 65, 70, 75, 80Zr (at%)	Melting → casting → ± heat treatment	Ti-25, 50, 75Zr: α' (deduced from the martensitic structures)	—	Ti-50Zr had the greatest hardness and ultimate tensile strength	—	—
Ikarashi et al.	Ti-50at%Zr	Melting → casting	—	—	—	—	Ti-50Zr had better *in*

(2005) [38]							*vivo* biocompatibility than Ti
Lee et al. (2016) [30]	Ti-10, 20, 30, 40, 50, 60, 70, 80, 90Zr (at%)	Melting → casting	α	—	Ti-30Zr had the highest ultimate tensile strength and hardness, and a low elastic modulus.	—	Ti-50Zr had a decreased biological response than Ti
Akimoto et al. (2016) [31]	Ti-30, 50, 70Zr (at%)	Melting → casting	α*	—	—	Ti-30, -50Zr had higher corrosion resistance	—
Tan et al. (2022) [39]	Ti-10, 30, 50Zr (at%)	Melting → casting	α*	Sandblasting and acid etching	—	—	Cell attachment and Ca deposition: treated Ti-10, -30Zr, Ti > treated Ti-50Zr
Zhao et al. (2022) [40]	Ti-30Zr (at%)	Melting → casting	α*	Sandblasting and H₂SO₄/H₂O₂ treatment	—	—	Cell attachment: treated Ti-30Zr > treated Ti
Wang et al. (2018) [13]	Ti-5, 15, 25, 35, 45Zr (wt%)	Powder mixing → compacting → sintering	α and α'	—	Ti-45Zr had the maximum bending strength and compressive strength, and a low elastic modulus.	—	All the alloys had a good cell attachment and spreading
Ou et al. (2021) [36]	Ti-5, 15, 25, 35, 45Zr (wt%)	Powder mixing → compacting → sintering	α and α'*	—	The same as above	Corrosion resistance: Ti-Zr alloys > Ti	Ti-45Zr showed good cytocompatibility and osteogenic activity than Ti
Ou et al. (2022) [37]	Ti-45wt%Zr	Powder metallurgy	α and α'	—	—	—	Ti-45Zr had good *in vivo* biocompatibility and osteointegration
Bolat et al. (2012) [33]	Ti-55, 75, 95Zr (wt%)	—	—	—	—	Ti-55Zr was corrosion-resistant in Ringer's solution	—
Bolat et al. (2013) [34]	Ti-55, 75, 95Zr (wt%)	—	—	Thermal oxidation	—	Oxidized Ti-55Zr had the highest corrosion resistance in Ringer's solution	—
Mareci et al. (2013) [32]	Ti-55, 75, 95Zr (wt%)	—	α	—	—	Ti-75Zr and Ti-95Zr were susceptible to localized corrosion in artificial saliva with different contents	—
Mareci et al. (2014) [35]	Ti-55, 75, 95Zr (wt%)	Electron beam melting → casting	—	Thermal oxidation	—	Oxidized Ti-95Zr had the highest corrosion resistance in fluoride-containing environments	—
Sista et al. (2011) [41]	Ti-50wt%Zr	Powder consolidation → sintering	—	—	—	—	Ti-50Zr had a comparable biological performance to Ti
Sista et al. (2012) [42]	Ti-50wt%Zr	Powder consolidation → sintering	—	—	—	—	Ti-50Zr showed higher expression of cell-matrix adhesion- and differentiation-related genes than Ti

Same-color rows: Studies by the same or related researchers.

*The deduced phase composition. The phase composition was not directly measured in the study but was inferred from their previous studies because the same alloys were produced through the same method by the same research team.

UTS, ultimate tensile strength; YS, yield strength; EL, elongation; SLA, large grit sandblasting and acid etching.

binary Ti-Zr alloy) [12]. It can be seen that the phase transformation starting temperature decreases with an increase in Zr content up to 50 at. % [13], indicating that in this range, during the cooling phase transformation, the α phase growth was inhibited.

Table 1 shows that the α or α′ phase (complete or martensitic transformation from the β phase) may be achieved in Ti-Zr alloys with zirconium concentrations of the full range, regardless of whether the raw materials are metal sponges or powder and the subsequent processing methods: hot swaging, forging, rolling, casting, or cold working, no matter their different heat treatments and different cooling conditions or cooling rates. The α phase of Ti-Zr alloys can probably be explained by the complete solid solution system of titanium and zirconium [13]. By contrast, α′ phase formation is a shear mechanism that proceeds through the processes of atom movement and lattice deformation [16]. For Ti-Zr alloys with the same composition, at low cooling rates, a complete α single phase can be obtained. By contrast, during fast cooling from the temperature range of β phase stability, martensitic transformat. ion (α′ phase formation) proceeds [16]. As reported by Kobayashi et al., to obtain a completely homogeneous α single-phase structure in Ti-Zr alloys containing 25, 50, and 75 at. % zirconium, 0.1 degree/s cooling would be needed rather than the faster 1.0 degree/s, which induced martensitic transformation [17]. The martensitic α′ phase has typical microstructures such as lamellae and needles. In addition, Zr concentration increase results in the thinner and increased number of lamellae and needle structures [13].

Three studies have reported their Ti-Zr alloys as two-phase α + β alloys [18–20]. Kim et al. found that after homogenization at 1000 °C for 24 h, Ti- (10, 20, 30, and 40 wt. %) Zr showed the diffraction peaks corresponding to α and β phases by XRD (X-ray diffraction spectra). Each diffraction peak shifts to a lower angle with an increasing Zr content [18]. It is noticeable that this homogenization condition is the same as that in the study by Kobayashi et al. (1273 K, 86.4 ks) [17], where Ti-(25, 50, and 75 at. %) Zr showed a martensitic structure but no β phase structures. Besides, before the same heat treatment (homogenization), all the alloys in both studies had undergone a melting process, and the Ti-25at (38.8 wt. %) Zr in the study by Kobayashi et al. had a very close composition ratio with the Ti-40 wt. %Zr by Kim et al. Generally, whether α/β allotropic transformation or some kind of diffusionless transformation occurs is determined the balance of diffusibility, which depends on the transformation temperature and cooling rate [17]. Because the transformation temperature is determined by the composition of Ti-Zr alloys, as shown in Fig. 3, both studies have similar Ti and Zr composition ratios. Therefore, the phase difference for both studies

can be attributed to the different cooling rates, although Kim et al. did not describe their cooling condition. The XRD peaks shifting toward the low-angle side is because of the larger atomic radius of Zr (1.62 Å) than that of Ti (1.47 Å). Thus, the addition of zirconium caused lattice parameters to increase [21].

Hsu et al. found that Ti-90 wt. %Zr comprised only the α′ phase, Ti-(70 and 80 wt. %)Zr comprised α′+ β phases, whereas Ti-60 wt. %Zr comprised only the β phase [19]. All procedures were the same for the alloys in their study; therefore, the phase diversity should result from the different zirconium percentages because the α/β transformation temperature changes with the zirconium composition in Ti-Zr alloys [12]. The authors explained that the β phase retained in Ti-(60, 70, and 80 wt. %) Zr at room temperature was because the Ms temperature became lower than room temperature with the addition of titanium to zirconium. They also emphasized the effect of their fast cooling condition [17], which can be suggested from the only α′ phase in the Ti-90 wt. %Zr because the α′ phase is prone to form under fast cooling conditions. It should be clarified that the experimental Ms temperature was lower than the room temperature [19], but, the Ms temperature is approximately 500 °C if referring to Fig. 3. This temperature gap was also reported previously, where the Ms of Ti-10 wt. %Zr was approximately 180 °C and significantly lower than the reference temperature of 805 °C. This was possibly because of the deviation in the determination method for the Ms temperature [12]. In addition, impurities also affect phase transformation. Of these three studies [18–20], only Moreno et al. provided information on the elemental composition of their raw materials. Although Fe, Mo, W, Ni, and Nb are β-stabilizers, the other impurities C, N, and O are α-stabilizers. Therefore, the decreasing effect of β-stabilizers and the increasing effect of α-stabilizers on α/β transus temperature may have been balanced in their study. Moreover, the effect of impurities on Ms temperature was reported very small, where the addition of 0.11 wt. %Fe only lowered 20 °C of Ms [12]. Therefore, the impurity effect cannot explain the large Ms temperature gap.

However, different processing conditions can also cause differences in microstructures. Imgram et al. varied the alloy (Ti-5, 10, 15, 20, and 40 wt%Zr) structures by combining hot working (forging and swaging) and heat treatment (annealing and quenching). Ti-20. and 40 wt. %Zr exhibited α + β phases caused by swaging above the α/β transition temperature. Further heat treatments were even able to modify the proportion and microstructure of the retained β phase in the same alloy under different conditions (equiaxed α + β, β-quenched, β-furnace-cooled) [22]. Moreno et al. found a Ti-20 wt. %Zr alloy produced by vacuum semi-levitation melting consisting of α and β phases. There is no information about their additional procedures; however, they also mentioned that diffusion-controlled nucleation and the growth of the α-phase structure into β-grains were led by the slow and intermediate cooling process (< 1 K/s), which started from the homogenization temperature [20].

In this section, as illustrated in Fig. 4, it can be concluded that the phase composition and microstructure of Ti-Zr alloys are determined by the Zr and Ti contents in the alloy and various manufacturing methods.

4.2. Mechanical, chemical corrosion, and electrochemical corrosion resistance properties

Analyzing the microstructure is important because the mechanical and corrosion resistance properties depend fundamentally on the microstructure features [23,24]. To extract an optimal composition ratio of Zr in Ti-Zr alloys, it is essential to compare the testing data for alloys of the same phase. As shown in Table 1 (green rows), all alloys are in the α or α′ phase. Cordeiro et al. found that all Ti-Zr alloys (5, 10, and 15 wt. %Zr) had statistically more significant hardness than that of Ti or even Ti-6Al-4 V. The increase in the hardness of Ti-Zr alloys is a consequence of solid-solution hardening
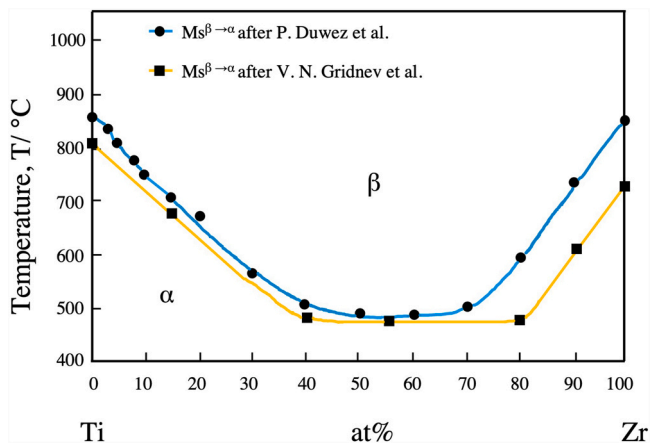

Fig. 3. Phase diagram of Ti-Zr binary alloy system adapted from Fig. 1 in the study of Kobayashi et al. [12]; the blue line with Ms points adapted after Duwez et al. [14]; the yellow line with Ms points plotted after Gridnev et al. [15].
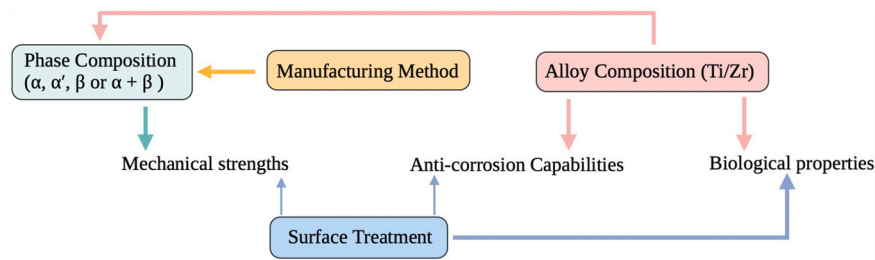
Fig. 4. Relationship diagram of influencing factors regarding binary Ti-Zr alloy. Alloy composition, manufacturing method, phase composition and surface treatment have their respective effects on mechanical, corrosion resistance and biological properties. The two different thicknesses of the arrows indicate the primary determining role, and the secondary influencing role, respectively.

generated by the α phase and grain refining caused by the thermo-mechanical process (homogenization and air cooling) [23–25]. By contrast, Correa et al. found no difference in hardness for Ti-5, 10, 15 wt. %Zr, and Ti and explained that this might be related to the effect of the residual stresses of the processing on the atomic mobility [26]. It can be concluded that the contribution to hardness increase made by heat treatment and air cooling is essential because the Ti-Zr alloys (5, 10, and 15 wt. %Zr) did not show significantly different hardness with Ti when there was no further process after hot swaging in the study of Correa et al. [26] compared with the studies of Cordeiro et al. [23,24] and Barão et al. [25]. In addition to the hardness, the elastic modulus related to alloy hardening was also increased by the processes performed after swaging. The elastic modulus is determined by the bonding force between atoms, which is not only related to the crystal structures but also to the distances between the atoms. The addition of alloying elements, heat treatment, and plastic deformation can all change the bonding force [26]. Because the Zr atomic radius is larger than the Ti atomic radius, increasing the Zr content in the alloy must lead to increasing degrees of supersaturation and lattice distortion, which also changes the distance between the atoms and results in a change in the elastic modulus. Therefore, for Ti-Zr alloys with the same α phase, the variation in the elastic modulus should result primarily from the different Zr contents.

A high elastic recovery capability, indicating a high strength and low modulus, is essential for many load-bearing implants and dental applications [26]. Implant materials with lower elastic moduli (closer to that of human bone) can reduce the stress-shielding effect [13]. Accordingly, Ti-Zr alloys with low moduli are preferable for implant materials. From Table 1 (green rows), it can be concluded that Ti-5 wt. %Zr has the lowest elastic modulus. Regarding the chemical and electrochemical corrosion resistance capability, Ti-5 and −15 wt. %Zr performed the best [23–25,27]. Corrosion resistance is a significant factor that influences the longevity of implants and the harmfulness of the corrosion processes occurring in the body. The improved corrosion resistance of Ti-Zr binary alloys can be attributed to the fact that Zr is an anodic alloying element for Ti that directly reduces the anodic activity.

The main reason for the electrochemical superiority of the alloys was related to a thicker and denser passive film on the Ti-Zr alloy surfaces that were reinforced by the ZrO_2 oxide [23]. In the study by Cordeiro et al., Ti-5 wt. %Zr showed the largest diameter on the Nyquist plot, indicating that its oxide layer is a better capacitor and is more protective. Similarly, the Bode plot results corroborate the higher protective properties of the oxide film of Ti-5 wt. %Zr. The authors explained that because the solid-solution strengthening of the alloy may be responsible for the enhanced protection against oxidation, the greater corrosion protection of Ti-5 wt. %Zr could also be justified by its largest hardness. In the EIS (electrochemical impedance spectroscopy) results, Ti-5 wt. %Zr showed low I_{corr} (corrosion current density), and $I_{pass\ (passivation\ current\ density)}$ values, which reflected low electrochemical activity and high corrosion resistance

properties [23]. In their another study, Ti-5 wt. %Zr presented the noblest behavior in the machined group as its open-circuit potential shifted to more electropositive values than that of the other alloys. Moreover, the acid-etching treatment significantly enhanced the electrochemical potential of all the materials, indicating a lower tendency to lose electrons to the environment. On analyzing the EIS, electrical parameters of the equivalent circuit models and polarization curves, Ti-Zr alloys exhibited a more resistant and protective oxide layer than Ti. The double etching increased the polarization resistance and E_{corr} (corrosion potential) to more electropositive values, which suggested an improvement in the corrosion protection tendency and higher stability of the oxide layer. The Ti-15 wt. %Zr alloy presented notably lower capacitance, I_{corr}, and I_{pass} values, which was probably related to the fact that the presence of Zr oxides is proportional to the Zr concentration in the alloy [24]. As shown in Table 1 (green rows), it was probably revealed that the suitability of implant material selection in decreasing order is Ti-5 wt. %Zr, Ti-15 wt. %Zr, Ti, and Ti-10 wt. %Zr [25].

Although both Ho et al. [21] and Kim et al. [18] investigated Ti-(10, 20, 30, and 40 wt. %)Zr alloys, the Ti-Zr alloys were α and α + β phases, respectively. Among the alloys of their respective phases, the α phase-Ti-40 wt. %Zr alloy showed the highest hardness value, bending strength, and elastic recovery capability, and the α + β phase-Ti-40Zr showed the highest corrosion resistance. Hsu et al. found that the hardness of the Ti-90 wt. %Zr alloy with an α′ phase was significantly higher than that of the Ti-60 wt. %Zr alloy containing only the β phase, which agrees with the fact that the β-phase alloy has the lowest hardness in the Ti-Nb system reported by Lee et al. [28]. Ti-90 wt. %Zr also exhibited a low modulus, excellent elastic recovery capability, and impressive strength [19].

Cui et al. studied the mechanical and chemical properties of Ti-Zr alloys under different surface treatments, zirconium contents, and manufacturing methods. The hardness of Ti-60 wt. %Zr and Ti-80 wt. %Zr was significantly improved after the thermal oxidation treatment (500 °C, 2 h), which was evidently attributed to the thick and compact ZrO_2 or $ZrTiO_4$ coatings formed by the treatment because ZrO_2 and $ZrTiO_4$ have much higher hardness compared to the Ti-Zr substrates. Moreover, ZrO_2 and $ZrTiO_4$ coatings have high chemical stability in fluoride-containing oral environments and even in acidic media, significantly decreasing the risk of pitting corrosion. Good mechanical properties of the coatings are important for decreasing the wear rate. Oxidized Ti-60 wt. %Zr and Ti-80 wt. %Zr showed higher corrosion resistance than that of the un-oxidized ones, and oxidized Ti-60 wt. %Zr had the best corrosion resistance and wear resistance [1]. In their another study, hot-rolled Ti-50 wt. %Zr implants endured higher loads than commercial cold-working Ti-16 wt. %Zr implants in air and artificial saliva solutions. Compared to smooth surfaces, SLA-treated surfaces had a harmful effect on the fatigue performances of Ti-16 wt. %Zr and Ti-50 wt. %Zr, indicating that although sandblast treatment produces a surface-hardened layer that is beneficial to the improvement of fatigue performance, micro-dimple defects formed by acid etching after sandblasting

accelerate fatigue cracking. Nevertheless, the fatigue limit of the SLA-treated Ti-50 wt. %Zr implant was still higher than that of the smooth surface Ti-16 wt. %Zr [29].

Kobayashi et al. studied Ti-20–80at. %Zr alloys. Microstructures of Ti-25, 50, and 75at. %Zr were compared via optical microscopy. Some types of martensitic structures were observed on both the as-cast and homogenized alloys, and no great differences were found between the as-cast structures and as-homogenized structures. Therefore, they concluded that the hardness of Ti-Zr alloys was determined by alloy composition and not by heat treatment because no differences in hardness were measured between the as-cast and as-homogenized alloys. However, Ti-50at. %Zr had the highest hardness (as-cast is approximately 230 HV) and ultimate tensile strength (approximately 920 MPa) [17].

Lee et al. [30] examined Ti-10–90at. %Zr alloys (as-cast). They found that Ti-30at. %Zr had the highest ultimate tensile strength (980 MPa), hardness (301 HV), and low elastic hardness (90 E/GPa), whereas Ti-50at. %Zr had a smaller ultimate tensile strength of 820 MPa and hardness of approximately 280 HV. Comparing the largest testing data of both studies, those of Lee et al. were slightly higher than those of Kobayashi et al., which may be owing to the different initial oxygen contents and other impurities in the raw titanium and zirconium. Because the hardness values of titanium were 128 HV (Lee et al.) and 110 HV (Kobayashi et al.), it is understandable that the testing values of the alloys were different in these two studies. It has also been proposed that an additional increase in the hardness of the solid solution was caused by a greater quantity of oxygen in Ti-5 and −10 wt. %Zr [26]. After Lee et al., Akimoto et al. further investigated the anti-corrosion capability of Ti-30, 50, and 70at. %Zr and found that Ti-30 at. % (i.e. 45 wt. %) and 50at. %Zr were more corrosion resistant, as Ti-70 at. % and Zr were observed pitting-corrosion. Moreover, their XPS (X-ray photoelectron spectroscopy) result also showed a Zr-rich passive layer is formed on these Ti-Zr alloys [31].

Wang et al. prepared Ti-5, 15, 25, 35, and 45 wt. %Zr alloys by a way of powder metallurgy and verified that their alloys were all in the α and α′ phases. Both the bending strength and compressive strength obviously improved with increasing Zr content, and the Ti-45 wt. %Zr alloy exhibited the maximum values. The improvement in compressive and bending strengths produced by alloying was probably induced by two aspects: the solid solution mechanism and grain refinement effect. First, both the α and β phases exhibited a complete solid solution without the presence of an intermetallic compound. The solid-solution mechanism produces a greater obstacle to the slip system, increasing the mechanical properties. Second, gradual progress in grain refinement was observed. Grain refinement causes an increase in the grain boundary area, which causes great resistance in the dislocation glide, resulting in improved mechanical properties [13].

Mareci and Bolat et al. tested the corrosion resistance capability of Ti-55, 75, and 95 wt. %Zr under various conditions. Ti-55 wt. %Zr exhibited the best corrosion resistance capability in artificial saliva, saliva +0.1 % fluoride ions pH = 5.6, saliva + 0.1% fluoride ions + lactic acid pH = 3.4, saliva + 0.1% fluoride ions + lactic acid + 0.6 % albumin pH = 3.4, and Ringer's solution [32–34]. However, in high fluoride-ion-containing environments (acidic artificial saliva + NaF concentrations 0.2, 0.5, and 1 wt. % pH = 3), the oxidized Ti-95 wt. %Zr was more corrosion resistant (the slowest corrosion rates, smallest passivating currents, and no sign of breakdown of the passive film up to +1.0 V_{SCE}) (SCE, saturated calomel reference electrode) than the other alloys after the thermal oxidation treatment (500 °C, 2 h) [35]. They showed it is very obvious that the trend of corrosion resistance with increasing Zr content in Ti-Zr alloys is the opposite between high-chloride-containing and high-fluoride-ion-containing environments [34]. This phenomenon may be related to the poor resistance of TiO_2 to fluoride ions. On the surfaces of Ti-55 and 75 wt. %Zr, there

were more Ti contents reacting with fluoride ions, so the less Ti-contained Ti-95 wt. %Zr exhibited more resistance. However, in both cases (high chloride-containing and high fluoride-ion-containing environments), the thermal oxidation treatment (500 °C, 2 h) improved the corrosion resistance of Ti-Zr alloys [35].

In this section, as illustrated in Fig. 4, it can be concluded that the mechanical properties of Ti-Zr alloys primarily depend on the phase composition and microstructure, and their anti-corrosion capabilities are mainly determined by the zirconium and titanium composition of the alloy. Surface treatments can also influence mechanical and anti-corrosion properties. For instance, double etching can improve the corrosion protection and stability of the oxide layer [24], and thermal oxidation treatment (500 °C, 2 h) can improve the hardness and chemical stability, thus decreasing the wear rate [1].

4.3. Biocompatibility, osteogenesis, osteointegration, and surface treatment

Biocompatibility is an essential aspect of dental implants, which describes the tendency of the implant to not cause toxic, allergic, or inflammatory responses *in vivo*. Ions released from dental implants can cause adverse reactions. It was reported that Ti ions are the causative factor of peri-implant mucositis, which can further induce severe peri-implantitis with alveolar bone resorption [11,36]. In this regard, the high corrosion resistance of Ti-Zr alloys is an absolute advantage over Ti implants. Comparisons of the corrosion resistance are discussed above. The *in vitro* biocompatibility results are presented herein.

Correa et al. found that Ti-5, 10, and 15 wt. %Zr alloys did not exhibit noticeable cytotoxic effects on MC3T3-E1 cells [26]. There was no statistically significant difference in albumin adsorption on Ti-5, 10 wt. %Zr, and Ti [23] and in MC3T3-E1 cell adhesion and proliferation on Ti-5, 10, 15 wt. %Zr, and Ti [24]. Wang et al. also found their Ti-Zr alloys (Ti-5, 15, 25, 35, and 45 wt. %Zr) surfaces had no cellular cytotoxicity and supported cellular attachment and spreading of MG-63 cells [13]. Through their further study, Ou et al. concluded that Ti-45 wt. %Zr showed better cytocompatibility than that of Ti and higher osteogenic activity than that of the other alloys. Here, it is particularly worth mentioning that, compared to Ti, the expression levels of osteogenesis-related genes were significantly lower on Ti-15Zr alloy, but not significantly lower or even higher on Ti-45Zr alloy [36]. They also investigated biocompatibility, osteointegration ability, and immune response effects of Ti-45 wt. %Zr in animal experiments. The results showed that Ti-45 wt. %Zr had good blood compatibility and was beneficial to the balance of macrophage polarization, which is important for host response and the long-term stability of osteointegration. The Ti-45 wt. %Zr alloy had direct contact with bone tissue without an obvious fibrous layer formed in between, presenting a good osteointegration ability in rabbit animal models. The osteointegration ability of an implant material is related to many factors, including composition elements, elastic modulus, surface properties, porosity, and pore size. Therefore, the good osteointegration ability of Ti-45 wt. %Zr may be attributed to its composition (Ti and Zr) and excellent mechanical properties (low elastic modulus) [37].

Ikarashi et al. evaluated the tissue response and development of metal sensitization by placing the samples in a subcutaneous position in rats for 8 months and found that the tissue inflammatory responses to Ti-50at. %Zr alloy were lower than those to Ti and no sensitization response to the alloy [38]. However, Lee et al. found that Ti-50at. %Zr had a significantly lower initial cell attachment rate and smaller cell size of MC3T3-E1 cells than those of Ti [30]. Similarly, Tan et al. found that SLA-treated Ti-50at. %Zr had the lowest cell attachment level after 6 h of MC3T3-E1 cell culture and the lowest Ca deposition on days 21 and 28, whereas SLA-treated Ti-

10 at. % Zr had more Ca deposition than Ti-30 and 50at. %Zr on day 21 [39]. Therefore, these results may suggest that while Ti-50at. %Zr had a smaller tendency to induce inflammatory responses because of the lower release of ions owing to its higher anti-corrosion capability, Ti-50at. %Zr alloy is less osteogenic than Ti. Moreover, Zhao et al. modified Ti-30at. %Zr and Ti with H_2SO_4/H_2O_2 to achieve micro/submicron/nano-structured surfaces and found that the MC3T3-E1 cell attachment level after 6 h and 24 h on Ti-30at. %Zr was superior to that of Ti [40].

Sista et al. compared Ti-50 wt. %Zr, Ti-50 wt. %Nb, and Ti; Ti-50 wt. %Zr showed better initial cell attachment, viability, proliferation, and differentiation (ALP activity and OC staining) of MC3T3 than Ti or Ti-50 wt. %Nb. They attributed the superior cell adhesion and proliferative activity on Ti-Zr to the synergistic effect of the surface energy and surface roughness. Regarding differentiation, which is influenced by the topography, roughness, and composition of the material surface, the author considered that the differences in cell differentiation on Ti-50 wt. %Zr and Ti-50 wt. %Nb surfaces are due to the different chemical compositions of the two Ti alloys [41]. In their another study, the expression of adhesion-supporting genes and differentiation-related genes on the Ti-50 wt. %Zr surface was higher than that of Ti, further verifying the influence of the substrate composition on osteoblast differentiation [42].

In this section, as illustrated in Fig. 4, it can be concluded that the biocompatibility, osteogenesis, and osteointegration of Ti-Zr alloys are determined by the substrate chemical composition and surface treatments. On smooth surfaces, the chemical composition of Ti-Zr alloys plays a major role because surface properties (such as roughness and surface energy) that influence the interaction of the material with the cell and tissue are related to the substrate composition. Surface treatments have a great effect on biocompatibility, osteogenesis, and osteointegration because the surface morphology, roughness, energy, and chemical stability of the passive film can all be modified by applying different surface treatments based on the existing substrate composition.

5. Conclusions

The following conclusions can be drawn from the current literature.

The titanium and zirconium composition ratios in the binary alloys and the manufacturing process determine the produced phase composition and microstructure of Ti-Zr alloys.

The phase composition and microstructure of Ti-Zr alloys lead to different mechanical properties, whereas the chemical or electrochemical stability is primarily determined by the zirconium and titanium composition in the alloy. Surface treatments can influence both the mechanical and anti-corrosion properties.

The biocompatibility, osteogenesis, and osteointegration of Ti-Zr alloys are related to the chemical composition of the substrate and surface treatments.

Therefore, a good understanding of the phase, manufacturing process, and surface treatment is a prerequisite for controlling the mechanical, chemical, electrochemical, and biological properties of Ti-Zr alloys.

Examining Table 1 comprehensively, one can conclude that α or α′ phase-Ti-5 wt, 45 wt/30at, and 50 wt. %Zr have more promising results thus far, with better performance in terms of mechanical, chemical, electrochemical, and biological properties. However, information about Ti-Zr alloys of the α + β and β phases is insufficient to propose the composition ratio of titanium and zirconium.

Conducting more research may be considered to directly compare the studied binary alloys with the commercial Ti-15Zr in order to evaluate their possibility for use in new implants. More *in vitro* and *in vivo* results are necessary for these alloys to be considered as

potential substitutes for titanium and Roxolid Ti-15Zr for dental implant manufacturing.

Declaration of Competing Interest

Acknowledgements

References

[1] Cui WF, Shao CJ. The improved corrosion resistance and anti-wear performance of Zr-xTi alloys by thermal oxidation treatment. Surf Coat Technol 2015;283:101–7. https://doi.org/10.1016/j.surfcoat.2015.10.051

[2] Medvedev AE, Molotnikov A, Lapovok R, Zeller R, Berner S, Habersetzer P, et al. Microstructure and mechanical properties of Ti-15Zr alloy used as dental implant material. J Mech Behav Biomed Mater 2016. https://doi.org/10.1016/j.jmbbm.2016.05.008

[3] Lotz EM, Olivares-Navarrete R, Hyzy SL, Berner S, Schwartz Z, Boyan BD. Comparable responses of osteoblast lineage cells to microstructured hydrophilic titanium-zirconium and microstructured hydrophilic titanium. Clin Oral Implants Res 2017;28:e51–9. https://doi.org/10.1111/clr.12855

[4] Yin L, Chang Y, You Y, Liu C, Li J, Lai H-C. Biological responses of human bone mesenchymal stem cells to Ti and TiZr implant materials. Clin Implant Dent Relat Res 2019;21:550–64. https://doi.org/10.1111/cid.12756

[5] Kammerer PW, Palarie V, Schiegnitz E, Hagmann S, Alshihri A, Al-Nawas B. Vertical osteoconductivity and early bone formation of titanium-zirconium and titanium implants in a subperiosteal rabbit animal model. Clin Oral Implants Res 2014;25:774–80. https://doi.org/10.1111/clr.12175

[6] Wen B, Zhu F, Li Z, Zhang P, Lin XN, Dard M. The osseointegration behavior of titanium-zirconium implants in ovariectomized rabbits. Clin Oral Implants Res 2014;25:819–25. https://doi.org/10.1111/clr.12141

[7] Ioannidis A, Gallucci GO, Jung RE, Borzangy S, Hammerle CHF, Benic GI. Titanium-zirconium narrow-diameter versus titanium regular-diameter implants for anterior and premolar single crowns: 3-year results of a randomized controlled clinical study. J Clin Periodo 2015;42:1060–70. https://doi.org/10.1111/jcpe.12468

[8] Grandin HM, Berner S, Dard M. A review of titanium zirconium (TiZr) alloys for use in endosseous dental implants. Mater (Basel) 2012;5:1348–60. https://doi.org/10.3390/ma5081348

[9] Schiegnitz E, Al-Nawas B. Narrow-diameter implants: a systematic review and meta-analysis. Clin Oral Implants Res 2018;29:21–40. https://doi.org/10.1111/clr.13272

[10] Ezugwu EO, Batista Da Silva R, Falco Sales W, Rocha Machado A. Overview of the machining of titanium alloys vol. 2. Elsevier; 2017. https://doi.org/10.1016/B978-0-12-409548-9.10216-7

[11] Wachi T, Shuto T, Shinohara Y, Matono Y, Makihira S. Release of titanium ions from an implant surface and their effect on cytokine production related to alveolar bone resorption. Toxicology 2015;327:1–9. https://doi.org/10.1016/j.tox.2014.10.016

[12] Kobayashi Sengo, Nakai Kiyomichi OY. Analysis of phase transformation in a Ti-10mass% Zr Alloy by hot stage optical microscopy 2001:2398–405.

[13] Wang B, Ruan W, Liu J, Zhang T, Yang H, Ruan J. Microstructure, mechanical properties, and preliminary biocompatibility evaluation of binary Ti–Zr alloys for dental application. J Biomater Appl 2019. https://doi.org/10.1177/0885328218811052

[14] Duwez PJ. Inst Met 1952;80:525–7.

[15] Gridnev VN, Trefilov VI, Minakov VN. Sov Phys Dokl 1960;5(6):1094–6.

[16] Motyka M, Kubiak K, Sieniawski J, Ziaja W. Phase transformations and characterization of α + β titanium alloys vol. 2. Elsevier; 2014. https://doi.org/10.1016/B978-0-08-096532-1.00202-8

[17] Kobayashi E, Matsumoto S, Doi H, Yoneyama T, Hamanaka H. Mechanical properties of the binary titanium-zirconium alloys and their potential for biomedical materials. J Biomed Mater Res 1995. https://doi.org/10.1002/jbm.820290805

[18] Kim WG, Choe HC. Nanostructure and corrosion behaviors of nanotube formed Ti-Zr alloy. Trans Nonferrous Met Soc CHINA 2009;19:1005–8. https://doi.org/10.1016/S1003-6326(08)60396-9

[19] Hsu H-C, Wu S-C, Sung Y-C, Ho W-F. The structure and mechanical properties of as-cast Zr-Ti alloys. J Alloy Compd 2009;488:279–83. https://doi.org/10.1016/j.jallcom.2009.08.105

[20] Moreno JMC, Popa M, Ivanescu S, Vasilescu C, Drob SI, Neacsu EI, et al. Microstructure, mechanical properties, and corrosion resistance of Ti-20Zr alloy in undoped and NaF doped artificial saliva. Met Mater Int 2014;20:177–87. https://doi.org/10.1007/s12540-013-6031-x

[21] Ho WF, Chen WK, Wu SC, Hsu HC. Structure, mechanical properties, and grindability of dental Ti-Zr alloys. J Mater Sci Mater Med 2008. https://doi.org/10.1007/s10856-008-3454-x

[22] Imgram AG, Williams DN, Ogden HR. Tensile properties of binary titanium-zirconium and titanium-hafnium alloys. J Less-Common Met 1962;4:217–25.

[23] Cordeiro JM, Beline T, Ribeiro ALR, Rangel EC, da Cruz NC, Landers R, et al. Development of binary and ternary titanium alloys for dental implants. Dent Mater 2017;33:1244–57. https://doi.org/10.1016/j.dental.2017.07.013

[24] Cordeiro JM, Faverani LP, Grandini CR, Rangel EC, da Cruz NC, Nociti Junior FH, et al. Characterization of chemically treated Ti-Zr system alloys for dental implant application. Mater Sci Eng C 2018;92:849–61. https://doi.org/10.1016/j.msec.2018.07.046

[25] Barão VAR, Ramachandran RA, Matos AO, Badhe RV, Grandini CR, Sukotjo C, et al. Prediction of tribocorrosion processes in titanium-based dental implants using acoustic emission technique: Initial outcome. Mater Sci Eng C Mater Biol Appl 2021;123:112000. https://doi.org/10.1016/j.msec.2021.112000

[26] Correa DRN, Vicente FB, Donato TAG, Arana-Chavez VE, Buzalaf MAR, Grandini CR. The effect of the solute on the structure, selected mechanical properties, and biocompatibility of Ti-Zr system alloys for dental applications. Mater Sci Eng C 2014;34:354–9. https://doi.org/10.1016/j.msec.2013.09.032

[27] Han MK, Hwang MJ, Yang MS, Yang HS, Song HJ, Park YJ. Effect of zirconium content on the microstructure, physical properties and corrosion behavior of Ti alloys. Mater Sci Eng A 2014;616:268–74. https://doi.org/10.1016/j.msea.2014.08.010

[28] LEE CM, JU JHCL CP. Structure–property relationship of cast Ti–Nb alloys. J Oral Rehabil 2002;29:314–22.

[29] Cui WF, Liu YH. Fatigue behavior of Ti50Zr alloy for dental implant application. J Alloy Compd 2019;793:212–9. https://doi.org/10.1016/j.jallcom.2019.04.165

[30] Lee TJ, Ueno T, Nomura N, Wakabayashi N, Hanawa T. Titanium-zirconium binary alloy as dental implant material: analysis of the influence of compositional change on mechanical properties and in vitro biologic response 2016;31:547–54. https://doi.org/10.11607/jomi.4349

[31] Akimoto T, Ueno T, Tsutsumi Y, Doi H, Hanawa T, Wakabayashi N. Evaluation of corrosion resistance of implant-use Ti-Zr binary alloys with a range of compositions. J Biomed Mater Res - Part B Appl Biomater 2018. https://doi.org/10.1002/jbm.b.33811

[32] Mareci D, Bolat G, Chelariu R, Sutiman D, Munteanu C. The estimation of corrosion behaviour of ZrTi binary alloys for dental applications using electrochemical techniques. Mater Chem Phys 2013;141:362–9. https://doi.org/10.1016/j.matchemphys.2013.05.024

[33] Bolat G, Izquierdo J, Santana JJ, Mareci D, Souto RM. Electrochemical characterization of ZrTi alloys for biomedical applications. Electro Acta 2013;88:447–56. https://doi.org/10.1016/j.electacta.2012.10.026

[34] Bolat G, Izquierdo J, Mareci D, Sutiman D, Souto RM. Electrochemical characterization of ZrTi alloys for biomedical applications. Part 2: the effect of thermal oxidation. Electro Acta 2013;106:432–9. https://doi.org/10.1016/j.electacta.2013.05.093

[35] Mareci D, Bolat G, Cailean A, Santana JJ, Izquierdo J, Souto RM. Effect of acidic fluoride solution on the corrosion resistance of ZrTi alloys for dental implant application. Corros Sci 2014;87:334–43. https://doi.org/10.1016/j.corsci.2014.06.042

[36] Ou PH, Hao C, Liu J, He RG, Wang BQ, Ruan JM. Cytocompatibility of Ti-xZr alloys as dental implant materials. J Mater Sci Med 2021;32. https://doi.org/10.1007/s10856-021-06522-w

[37] Ou P, Zhang T, Wang J, Li C, Shao C, Ruan J. Bone response in vivo of Ti-45Zr alloy as dental implant material. J Mater Sci Mater Med 2022;33:47. https://doi.org/10.1007/s10856-022-06664-5

[38] Ikarashi Y, Toyoda K, Kobayashi E, Doi H, Yoneyama T, Hamanaka H, et al. Improved biocompatibility of titanium-zirconium (Ti-Zr) alloy: Tissue reaction and sensitization to Ti-Zr alloy compared with pure Ti and Zr in rat implantation study. Nippon Kinzoku Gakkaishi/J Jpn Inst Met 2007⟨https://doi.org/10.2320/jinstmet.71.395⟩.

[39] TAN T, ZHAO Q, KUWAE H, UENO T, CHEN P, TSUTSUMI Y, et al. Surface properties and biocompatibility of sandblasted and acid-etched titanium–zirconium binary alloys with various compositions. Dent Mater J 2022;41:266–72. https://doi.org/10.4012/dmj.2021-210

[40] Zhao Q, Ueno T, Chen P, Nozaki K, Tan T, Hanawa T, et al. Fabrication of micro-/submicro-/nanostructured surfaces on Ti–Zr alloy by varying H_2SO_4/H_2O_2 treatment conditions and investigations of fundamental properties of a typical surface. Surf Interfaces 2022;34:102390. https://doi.org/10.1016/j.surfin.2022.102390

[41] Sista S, Wen C, Hodgson PD, Pande G. The influence of surface energy of titanium-zirconium alloy on osteoblast cell functions in vitro. J Biomed Mater Res - Part A 2011;97 A:27–36. https://doi.org/10.1002/jbm.a.33013

[42] Sista S, Wen C, Hodgson PD, Pande G. Expression of cell adhesion and differentiation related genes in MC3T3 osteoblasts plated on titanium alloys: Role of surface properties. Mater Sci Eng C 2013;33:1573–82. https://doi.org/10.1016/j.msec.2012.12.063